FINGERING FROM IONIZATION FRONTS IN PLASMAS[*]

MANUEL ARRAYÁS[†], SANTIAGO BETELÚ[‡], MARCO A. FONTELOS[§], AND
JOSÉ L. TRUEBA[†]

Abstract. In this paper we describe the formation of fingers from ionization fronts for a hydrodynamic plasma model. The fingers result from a balance between the destabilizing effect of impact ionization and the stabilizing effect of electron diffusion on ionization fronts. We show that electron diffusion acts as an effective surface tension on moving fronts and we estimate analytically the size of the fingers and its dependence on both the electric field and electron diffusion coefficient. We perform direct numerical simulation of the model and compute finger-like traveling waves analogous to structures such as Saffman–Taylor fingers and Ivantsov paraboloid in the context of Hele–Shaw and Stefan problems, respectively.

1. Introduction. Lightning is a stream of electrified air, known as plasma. Charged particles are bound in the air by powerful electric forces to form electrically neutral atoms and molecules. As a result, the air is an excellent insulator. This means that if we apply an electric field to a volume filled with neutral particles, electric currents will not flow. However, if a very strong electric field is applied to matter of low conductivity and some electrons or ions are created, then the few mobile charges can generate an avalanche of more charges by impact ionization. A low temperature plasma is created, resulting in an electric discharge. The change in the properties of a dielectric that causes it to become conductive is known as electric breakdown. Breakdown is a threshold process: no changes in the state of the medium are noticeable while the electric field across a discharge gap is gradually increased but, suddenly, at a certain value of the electric field, a current is detected.

Discharges can assume different appearances depending on the characteristics of the electric field and the properties of the medium. Phenomenologically, discharges can be classified into stationary ones, such as arc, glow, or dark discharges, and transient ones, such as sparks and leaders [18].

At atmospheric pressure and at distances over 1 cm between anode and cathode, the discharge channels are sharp and narrow, and we have a streamer discharge. A streamer is a sharp ionization wave that propagates into a nonionized gas, leaving a nonequilibrium plasma behind. Streamers have been also reported in early stages of atmospheric discharges [15, 17]. They can split into branches spontaneously, but how this branching is determined by the underlying physics is one of the greatest unsolved problems in the physics of electric discharges. The pattern of this branching resembles

---

[†]Area de Electromagnetismo, Universidad Rey Juan Carlos, Camino del Molino s/n, 28943 Fuenlabrada, Madrid, Spain (manuel.arrayas@urjc.es, joseluis.trueba@urjc.es).
[‡]Department of Mathematics, University of North Texas, P.O. Box 311430, Denton, TX 76203-1430 (betelu@unt.edu).
[§]Departamento de Matemáticas, Universidad Autónoma de Madrid, 28049 Cantoblanco, Madrid, Spain (marco.fontelos@uam.es).

1122

the ones observed in the propagation of cracks, dendritic growth and viscous fingering. Those phenomena are known to be governed by deterministic equations rather than by stochastic events. In this paper, we extend and generalize the results announced in [8] and implement direct numerical simulations of these deterministic models.

1.1. The minimal model for streamers. We consider a fluid description of a low-ionized plasma. The electron density N_e^d varies in time as

$$(1.1) \qquad \frac{\partial N_e^d}{\partial \tau^d} + \nabla_\mathbf{R}^d \cdot \mathbf{J}_e^d = S_e^d.$$

In this expression, the superscript d means that the quantity has physical dimensions so that τ^d is the physical time, $\nabla_\mathbf{R}^d$ is the gradient operator, S_e^d is the source term, i.e., the net creation rate of electrons per unit volume, and

$$\mathbf{J}_e^d(\mathbf{R}^d, \tau^d) = N_e^d(\mathbf{R}^d, \tau^d)\, \mathbf{U}_e^d(\mathbf{R}^d, \tau^d)$$

is the electron current density, with $\mathbf{U}_e^d$ being the average velocity of electrons. Similar expressions can be obtained for positive N_p^d and negative N_n^d ion densities. On timescales of interest for the case of negative streamers, the ion currents can be neglected because they are more than two orders of magnitude smaller than the electron one, so we will take

$$(1.2) \qquad \frac{\partial N_p^d}{\partial \tau^d} = S_p^d,$$

$$(1.3) \qquad \frac{\partial N_n^d}{\partial \tau^d} = S_n^d,$$

with $S_{p,n}^d$ being source terms for positive and negative ions. Conservation of charge has to be imposed in all processes so that the condition $S_p^d = S_e^d + S_n^d$ holds.

A usual procedure is to approximate the electron current $\mathbf{J}_e^d$ as the sum of a drift (electric force) and a diffusion term

$$(1.4) \qquad \mathbf{J}_e^d = -\mu_e \boldsymbol{\mathcal{E}}^d N_e^d - D_e^d \nabla_\mathbf{R}^d N_e^d,$$

where $\boldsymbol{\mathcal{E}}^d$ is the total electric field (the sum of the external electric field applied to initiate the propagation of a ionization wave and the electric field created by the local point charges) and μ_e^d and D_e^d are the mobility and diffusion coefficients of the electrons. Note that, as the initial charge density is low and there is no applied magnetic field, the magnetic effects in (1.4) are neglected. In principle, the diffusion coefficient is not completely determined but, in the case of equilibrium, diffusion is linked to mobility through the Einstein relation $D_e^d/\mu_e = kT/e$, with k being the Boltzmann constant, T the temperature, and e the absolute value of the electron charge.

Several physical processes can be considered to give rise to the source terms $S_{e,p,n}^d$. The most important of them are impact ionization (an accelerated electron collides with a neutral molecule and ionizes it), attachment (an electron may become attached when it collides with a neutral gas atom or molecule, forming a negative ion), recombination (of a free electron with a positive ion or a negative ion with a positive ion), and photoionization (when photons created by recombination or scattering processes interact with a neutral atom or molecule, producing a free electron and a positive ion; see [7] and references therein).

A model to describe streamers is obtained when explicit expressions for the source terms, the electron mobility μ_e, and the diffusion coefficient D_e^d are provided. It is also necessary to impose equations for the evolution of the electric field $\boldsymbol{\mathcal{E}}^d$. It is usual to consider that this evolution is given by Poisson's law,

$$(1.5) \qquad \nabla_{\mathbf{R}}^d \cdot \boldsymbol{\mathcal{E}}^d = \frac{e}{\varepsilon_0} \left(N_p^d - N_n^d - N_e^d \right),$$

where ε_0 is the permittivity of the gas and we are assuming that the absolute value of the charge of positive and negative ions is e.

A simplification occurs when the streamer development out of a macroscopic initial ionization seed is considered in a nonattaching gas such as argon or nitrogen [12]. In this case, attachment, recombination, and photoionization processes can be neglected. As a consequence, the negative ion density N_n^d can be considered constant. The balance equations turn out to be

$$(1.6) \qquad \frac{\partial N_e^d}{\partial \tau^d} = \nabla_{\mathbf{R}}^d \cdot \left(\mu_e \boldsymbol{\mathcal{E}}^d N_e^d + D_e^d \nabla_{\mathbf{R}}^d N_e^d \right) + \nu_i N_e^d,$$

$$(1.7) \qquad \frac{\partial N_p^d}{\partial \tau^d} = \nu_i N_e^d.$$

This is called the minimal streamer model for a nonattaching gas. In these equations, $\nu_i N_e^d$ is a model for the impact ionization source term, in which the ionization coefficient ν_i is given by the phenomenological Townsend's approximation,

$$(1.8) \qquad \nu_i = \mu_e |\boldsymbol{\mathcal{E}}^d| \alpha_0 e^{-\mathcal{E}_0/|\boldsymbol{\mathcal{E}}^d|},$$

where α_0 is the inverse of ionization length. The ionization length is the distance, on average, that a free electron travels before ionizing a molecule. The value of α_0 is proportional to the pressure of the ambient gas according to Townsend's theory [9]. $\mathcal{E}_0$ is the characteristic impact ionization electric field.

Townsend's approximation provides physical scales and intrinsic parameters for the model as long as only impact ionization is present in the gas. It is then convenient to reduce the equations to a dimensionless form. The natural units for nitrogen are functions of the gas pressure p (in bars). These units are the ionization length

$$(1.9) \qquad R_0 = \frac{1}{\alpha_0} = 2.3 \times 10^{-6} \, \text{m} \left(\frac{p}{1 \, bar} \right)^{-1},$$

as a length unit, the characteristic impact ionization field

$$(1.10) \qquad \mathcal{E}_0 = 2 \times 10^7 \, \text{V/m} \left(\frac{p}{1 \, bar} \right),$$

as an electric field unit, and the electron mobility

$$(1.11) \qquad \mu_e = 3.8 \times 10^{-2} \, \text{m}^2/(\text{V} \cdot \text{s}) \left(\frac{p}{1 \, bar} \right)^{-1},$$

as a unit of velocity divided by electric field. These natural units lead to the velocity scale

$$(1.12) \qquad U_0 = \mu_e \mathcal{E}_0 = 7.6 \times 10^5 \, \text{m/s},$$

the time scale

$$(1.13) \qquad \tau_0 = \frac{R_0}{U_0} = 3 \times 10^{-12}\,\mathrm{s}\left(\frac{p}{1\,bar}\right)^{-1},$$

the particle density scale

$$(1.14) \qquad N_0 = \frac{\varepsilon_0 \mathcal{E}_0}{eR_0} = 4.7 \times 10^{20}\,\mathrm{m}^{-3}\left(\frac{p}{1\,bar}\right)^{2},$$

and the electron diffusion scale

$$(1.15) \qquad D_0 = R_0 U_0 = 1.8\,\mathrm{m}^2/\mathrm{s}\left(\frac{p}{1\,bar}\right)^{-1}.$$

We introduce the dimensionless variables $\mathbf{r} = \mathbf{R}^d/R_0$, $\tau = \tau^d/\tau_0$, the dimensionless field $\boldsymbol{\mathcal{E}} = \boldsymbol{\mathcal{E}}^d/\mathcal{E}_0$, the dimensionless electron and positive ion particle densities $N_e = N_e^d/N_0$ and $N_p = N_p^d/N_0$, and the dimensionless diffusion constant $D_e = D_e^d/D_0$.

The dimensionless minimal model reads

$$(1.16) \qquad \frac{\partial N_e}{\partial \tau} = \nabla \cdot (N_e \boldsymbol{\mathcal{E}} + D_e\,\nabla N_e) + N_e |\boldsymbol{\mathcal{E}}| e^{-1/|\boldsymbol{\mathcal{E}}|},$$

$$(1.17) \qquad \frac{\partial N_p}{\partial \tau} = N_e |\boldsymbol{\mathcal{E}}| e^{-1/|\boldsymbol{\mathcal{E}}|},$$

$$(1.18) \qquad N_p - N_e = \nabla \cdot \boldsymbol{\mathcal{E}}.$$

This model exhibits spontaneous branching of the streamers, as indicated by numerical simulations [4], in agreement with experimental situations [17]. In order to understand this branching, Arrayás and Ebert [5] derived the dispersion relation for transversal Fourier-modes of planar negative shock fronts without diffusion (D_e). For perturbations of small wave number k, the planar shock front becomes unstable with a linear growth rate proportional to k. It has been also shown that all the modes with large enough wave number k (small wave length perturbations) grow at the same rate (the growth rate does not depend on k when k is large). However, it could be expected from the physics of the problem that a particular mode would be selected. To address this problem, we consider in this paper the effect of diffusion.

1.2. Outline of this paper. Our analysis will show that the electron density N_e may develop sharp fronts of thickness $O(\sqrt{D_e})$. Moreover, it satisfies an equation analogous to the Fisher equation, which is a well-known model in some biological contexts (see [14]). A surprising fact established during the last 30 years is that the combination of sharp interfaces with small diffusive effects may result in asymptotic limits (for $D_e \ll 1$) in which the motion of the interface is described by equations involving solely geometrical properties such as its mean curvature. A pioneer attempt to achieve such a description is due to Allen and Cahn [2] and concerns a model, today known as the Allen–Cahn equation, for the kinetics of melted Fe-Al alloys. Subsequent work by Rubinstein, Sternberg, and Keller [19] showed that the points of the interface separating both species move along the normal direction with a velocity proportional to its mean curvature. This kind of dynamics is termed "mean curvature flow." Many mathematicians have contributed to providing a rigorous proof of the convergence of the Allen–Cahn model to motion by mean curvature. These ideas have also been extended to some other, rather different, contexts. An improvement of the above model is the so-called Cahn–Hilliard model [10], described by a fourth

order differential equation. This model leads to an asymptotic limit given by the motion of sharp interfaces in the Hele–Shaw (or Mullins–Sekerka) problem for the evolution of a fluid between two plates separated by a small distance [1]. A biological model consisting of reaction-diffusion equations [11] for competing species separated by a sharp interface gives rise to a limiting problem similar to the Stefan problem for phase transformation (for example, ice solidifying water). Remarkably, some of these limiting models have solutions that develop branch-like patterns, such as fingers in Hele–Shaw or dendrites in the Stefan problem.

In this paper we exploit some of the ideas introduced in the references above in order to study the motion of ionization fronts. We will show that a planar front separating a partly ionized region from a region without charge is affected by two opposing effects: electrostatic repulsion of electrons and electron diffusion. The first effect tends to destabilize the front, while the second acts effectively as a mean curvature contribution to the velocity of the front that stabilizes it. The net result is the appearance of fingers with a characteristic thickness determined by the balance of these two opposing actions. The common underlying mathematical structure among the minimal streamer model and other pattern-forming systems such as the Hele–Shaw and Stefan problems strongly suggests that the basic mechanisms governing important phenomena such as the development of complex patterns through branching of single "fingers" should be very similar.

2. Streamer evolution in strong electric fields. In order to study the evolution and branching of ionization fronts, we consider the following experimental situation. The space between two plates is filled with a nonattaching gas such as nitrogen. A stationary potential difference is applied to these plates so that an electric field is produced in the gas. The electric field is directed from the anode to the cathode. To initiate the avalanche, an initial seed of ionization is set near the cathode. We study the evolution of negative ionization fronts towards the anode.

We will assume that the distance between the cathode and the anode is much larger than the space scale R_0 (in experiments, this distance is more than one thousand times larger than R_0) so that we can consider the anode to be at an infinite distance from the initial seed of ionization. Moreover, we will concentrate on the study of the dynamics under the effect of strong external electric fields, which are larger than the electric field unit $\mathcal{E}_0$. This means that the modulus of the dimensionless electric field $|\mathcal{E}|$ is larger than 1. Strictly speaking, if we denote by $\mathcal{E}_\infty$ the modulus of the dimensionless electric field at large distance from the cathode, we will assume that $\mathcal{E}_\infty \gg 1$. Under these circumstances, it is natural to rescale the dimensionless quantities in the minimal model as

(2.1) $$\boldsymbol{\mathcal{E}} = \mathcal{E}_\infty \, \mathbf{E},$$

(2.2) $$N_e = \mathcal{E}_\infty \, n_e,$$

(2.3) $$N_p = \mathcal{E}_\infty \, n_p,$$

(2.4) $$\tau = \frac{t}{\mathcal{E}_\infty},$$

so that we have

(2.5) $$\frac{\partial n_e}{\partial t} - \nabla \cdot (n_e \mathbf{E} + D \, \nabla n_e) = n_e |\mathbf{E}| e^{-1/(\mathcal{E}_\infty |\mathbf{E}|)},$$

(2.6) $$\frac{\partial n_p}{\partial t} = n_e |\mathbf{E}| e^{-1/(\mathcal{E}_\infty |\mathbf{E}|)},$$

(2.7) $$\nabla \cdot \mathbf{E} = n_p - n_e,$$

where

$$(2.8) \qquad D = \frac{D_e}{\mathcal{E}_\infty}$$

is, in general, a small parameter. For $\mathcal{E}_\infty \gg 1$, this system can be approximated by

$$(2.9) \qquad \frac{\partial n_e}{\partial t} - \nabla \cdot (n_e \mathbf{E} + D \nabla n_e) = n_e |\mathbf{E}|,$$

$$(2.10) \qquad \frac{\partial n_p}{\partial t} = n_e |\mathbf{E}|,$$

$$(2.11) \qquad \nabla \cdot \mathbf{E} = n_p - n_e.$$

Our approximation will be valid in all regions where $\mathcal{E}_\infty |\mathbf{E}| \gg 1$. These are the regions of interest in the situations studied in this paper since by (2.11) the intensity of the electric field varies continuously as long as n_e and n_p are bounded, and hence should not vary much in the neighborhood of the ionization front. We will show that this is indeed the case and it is in this region that the mechanisms leading to branching occur.

3. Planar fronts. We will concentrate on the planar case. Experimentally, this means that we have two large planar plates situated at $x = 0$ (cathode) and $x = d$ (anode), respectively (x is the horizontal axis and we suppose that $d \gg 1$). The space between the plates is filled with a nonattaching gas such as nitrogen. A stationary electric potential difference is applied to the plates so that an electric field is produced in the gas. The initial electric field is directed from the anode to the cathode and is uniform in the space between the plates with a value $\mathcal{E}_\infty \gg 1$. As in this section we are interested in the evolution of the ionization wave along the x axis, the rescaled electric field can be written as $\mathbf{E} = E \mathbf{u}_x$, where $E < 0$ so that $|\mathbf{E}| = |E| = -E$, and $\mathbf{u}_x$ is a unitary vector in the x direction. We are left then with the following system:

$$(3.1) \qquad \frac{\partial n_e}{\partial t} = \frac{\partial}{\partial x} \left(n_e E + D \frac{\partial n_e}{\partial x} \right) + n_e |E|,$$

$$(3.2) \qquad \frac{\partial n_p}{\partial t} = n_e |E|,$$

$$(3.3) \qquad \frac{\partial E}{\partial x} = n_p - n_e.$$

3.1. The traveling waves with $D = 0$. It is very simple to compute traveling wave solutions when $D = 0$. In this case, the equation for the evolution of the electron density is

$$(3.4) \qquad \frac{\partial n_e}{\partial t} = \frac{\partial (n_e E)}{\partial x} - n_e E.$$

Subtracting (3.1) from (3.2) with $D = 0$, and taking the time derivative of (3.3), we obtain the equation

$$(3.5) \qquad \frac{\partial^2 E}{\partial x \partial t} + \frac{\partial}{\partial x} (n_e E) = 0.$$

Integrating this expression once in x, one obtains

$$(3.6) \qquad \frac{\partial E}{\partial t} + n_e E = C(t),$$

where $C(t)$ can be fixed by the boundary conditions at infinity, $E \to -1$ and $n_e \to 0$. This implies $C(t) = 0$ so that

$$\text{(3.7)} \qquad \frac{\partial E}{\partial t} = -n_e E.$$

In physical terms, the left-hand side of (3.6), due to Ampére's law, is the curl of the magnetic field which is zero because the magnetic effects are neglected in the framework of the minimal model.

We look for traveling wave solutions of the system (3.4)–(3.7), introducing the ansatz

$$\text{(3.8)} \qquad n_e = f(x - ct), \ \ E = -g(x - ct)$$

into the above system. The minus sign in the electric field is due to the fact that the electric field is negative, so g is a positive function. Introducing (3.8) into (3.4) and (3.7), we obtain

$$\text{(3.9)} \qquad -c\frac{df}{d\xi} = \frac{d}{d\xi}(fg) + fg,$$

$$\text{(3.10)} \qquad c\frac{dg}{d\xi} = fg.$$

Introducing $dg/d\xi$ given by (3.10) into (3.9), we obtain an equation for $df/d\xi$, and hence we obtain the following system of ODEs:

$$\text{(3.11)} \qquad \frac{df}{d\xi} = \frac{-fg + \frac{1}{c}f^2 g}{c - g},$$

$$\text{(3.12)} \qquad \frac{dg}{d\xi} = \frac{1}{c}fg,$$

where $\xi = x - ct$. This system can be explicitly solved by noticing that

$$\text{(3.13)} \qquad \frac{df}{dg} = -\frac{c - f}{c - g}$$

so that

$$\text{(3.14)} \qquad (c - f)(c - g) = c(c - 1),$$

with the constant $c(c - 1)$ being given by conditions at $\xi \to \infty$, namely, that the electron density vanishes and the electric field is equal to -1 there. Therefore,

$$\text{(3.15)} \qquad \frac{dg}{d\xi} = \frac{g(1 - g)}{c - g},$$

allowing direct integration to yield the implicit solution (up to translations in ξ),

$$\text{(3.16)} \qquad c \log g + (1 - c) \log (1 - g) = \xi.$$

This expression yields solutions for any $c \geq 1$. We will be interested in the limit $c \to 1$ since it is well known [6] that compactly supported initial data (representing a seed
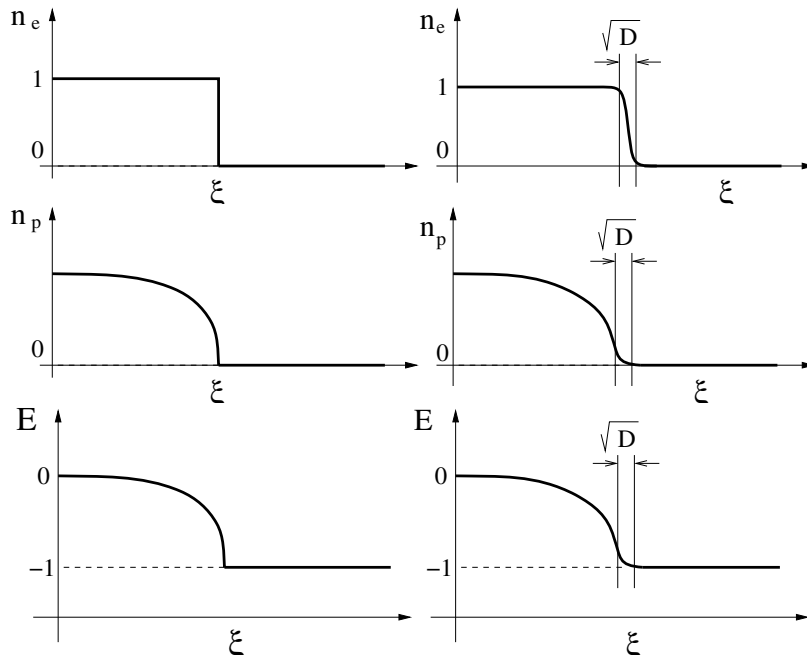
FIG. 1. *The moving fronts with $D = 0$ and $c = 1$. The moving fronts when $0 < D \ll 1$ and $c = 1 + 2\sqrt{D}$.*

of ionization located in some region) develop fronts traveling with this velocity. In the case $c = 1$ the solution can be obtained straightforwardly, giving

$$(3.17) \qquad g(\xi) = \begin{cases} e^{\xi}, & \text{for } \xi < 0, \\ 1, & \text{for } \xi \geq 0, \end{cases} \quad f(\xi) = \begin{cases} 1, & \text{for } \xi < 0, \\ 0, & \text{for } \xi \geq 0. \end{cases}$$

We can also find the solution for the positive ion density n_p in the case $c = 1$. Taking $n_p = h(x - t)$, we have

$$(3.18) \qquad h(\xi) = \begin{cases} 1 - e^{\xi} & \text{for } \xi < 0, \\ 0 & \text{for } \xi \geq 0. \end{cases}$$

This solution for n_e represents a shock front moving with velocity $c = 1$ (see Figure 1).

3.2. The traveling waves with $D \neq 0$. We proceed now to investigate the traveling waves for $0 < D \ll 1$. As D is a small parameter, the traveling wave solutions for the electron and positive ion densities and the electric field are expected to be not very different to that corresponding to $D = 0$ found in the previous subsection. Consequently, we look for solutions such that n_e and n_p decay exponentially at infinity and E is also an exponentially small correction of -1 at infinity. This means that we can take

$$(3.19) \qquad n_e = Ae^{-\lambda(x-ct)},$$
$$(3.20) \qquad n_p = Be^{-\lambda(x-ct)},$$
$$(3.21) \qquad E = -1 + Ce^{-\lambda(x-ct)}$$

asymptotically far behind the wave. If we introduce these expressions into (3.1) we obtain, for $x - ct \to \infty$, the relation

$$(3.22) \qquad\qquad -c\lambda + \lambda + D\lambda^2 = -1,$$

which has real solutions if and only if $(c-1)^2 - 4D \geq 0$. Therefore,

$$(3.23) \qquad\qquad c \geq 1 + 2\sqrt{D}.$$

All initial data decaying at infinity faster than $Ae^{-\lambda^* x}$, with $\lambda^* = 1/\sqrt{D}$, will develop traveling waves [12] with velocity $c = 1 + 2\sqrt{D}$. If $D \ll 1$, the profiles for n_p and E will vary very little from the profiles with $D = 0$. On the other hand, n_e will develop a boundary layer at the front, smoothing the jump from $n_e = 1$ to $n_e = 0$. If we write the equation for the traveling wave $n_e = f(x - (1 + 2\sqrt{D})t)$ into the expression

$$(3.24) \qquad \frac{\partial n_e}{\partial t} - n_e\frac{\partial E}{\partial x} - E\frac{\partial n_e}{\partial x} - D\frac{\partial^2 n_e}{\partial x^2} = n_e|E|,$$

and we take, from (3.3), $\partial_x E = n_p - n_e$, approximating at the boundary layer $n_p = 0$, $E = -1$, we obtain the equation

$$(3.25) \qquad -2\sqrt{D}\frac{\partial f}{\partial \xi} - D\frac{\partial^2 f}{\partial \xi^2} = f(1 - f),$$

where $\xi = x - (1 + 2\sqrt{D})t$. Defining $\chi = \xi/\sqrt{D}$, we obtain an equation for the boundary layer,

$$(3.26) \qquad -2\frac{\partial f}{\partial \chi} - \frac{\partial^2 f}{\partial \chi^2} = f(1 - f),$$

together with the matching conditions,

$$(3.27) \qquad\qquad f(-\infty) = 1, \ f(+\infty) = 0.$$

Expression (3.26) is the well-known equation for traveling waves of Fisher's equation. It appears in the context of mathematical biology [16] and is known to have solutions subject to (3.27). This means that we have a boundary layer of width $\sqrt{D}$ at $\xi = 0$ in which (3.26) gives the solution for the electron density n_e. Before this layer, we have $n_e \approx 1$, and after the layer, $n_e \approx 0$. When $D = 0$, this is the shock front found in the previous subsection. It will be useful to analyze the structure of n_p at the boundary layer. Introducing

$$(3.28) \qquad\qquad n_p = \sqrt{D}h(\chi),$$

one obtains from (3.2) the following formula at zero order in D, with $\chi = [x - (1 + 2\sqrt{D})t]/\sqrt{D}$:

$$(3.29) \qquad\qquad \frac{dh(\chi)}{d\chi} = f(\chi)$$

so that

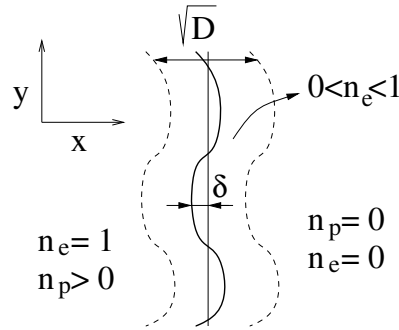$$(3.30) \qquad\qquad h(\chi) = -\int_\chi^\infty f(z)dz.$$

FIG. 2. *Schematic representation of the perturbed front.*

Notice that we now have

(3.31) $$\frac{\partial n_p}{\partial x} = f(\chi) = O(1) \text{ at the boundary layer.}$$

Analogously, from Poisson's equation $\partial_x E = n_p - n_e$, we can deduce $E = -1 + O(\sqrt{D})$ across the boundary layer. We will write this solution as

(3.32) $$E = -1 + \sqrt{D}E_{bl} + O(D).$$

These solutions can be seen in Figure 1.

4. The dispersion relation. The planar front studied in the previous sections may be unstable with respect to perturbations on the boundary layer, which then forms "ripples" or "corrugations." Consequently, we are interested in obtaining the dispersion relation to find which transversal mode will grow faster and eventually determine the characteristic shape of the streamer. So we let the planar front that propagates in the x-direction receive a small perturbation with an initial arbitrary dependence on the transversal coordinates.

Next we introduce a perturbation in the transversal direction y (see Figure 2). We will do it by introducing a new system of coordinates in the form

(4.1) $$\bar{t} = t,$$
(4.2) $$\bar{y} = y,$$
(4.3) $$\bar{x} = x - \delta\,\varphi(x, y, t)$$

so that, at $t = 0$, $n_e^{(0)}(\bar{x})$ and $E^{(0)}(\bar{x})$ correspond to the profiles of a traveling wave computed in the previous section, and δ is a sufficiently small parameter compared to $\sqrt{D}$. By doing this, we follow a strategy analogous to the one used in [19] to deduce the asymptotic approximation of the Allen–Cahn equation by mean curvature flow.

We can compute straightforwardly the relations between derivatives up to order δ^2,

$$\text{(4.4)} \qquad \frac{\partial}{\partial x} = \frac{\partial}{\partial \overline{x}} - \delta \frac{\partial \varphi}{\partial x} \frac{\partial}{\partial \overline{x}},$$

$$\text{(4.5)} \qquad \frac{\partial}{\partial y} = \frac{\partial}{\partial \overline{y}} - \delta \frac{\partial \varphi}{\partial y} \frac{\partial}{\partial \overline{x}},$$

$$\text{(4.6)} \qquad \frac{\partial}{\partial t} = \frac{\partial}{\partial \overline{t}} - \delta \frac{\partial \varphi}{\partial t} \frac{\partial}{\partial \overline{x}},$$

$$\text{(4.7)} \qquad \frac{\partial^2}{\partial x^2} = \frac{\partial^2}{\partial \overline{x}^2} - \delta \frac{\partial^2 \varphi}{\partial x^2} \frac{\partial}{\partial \overline{x}} - 2\delta \frac{\partial \varphi}{\partial x} \frac{\partial^2}{\partial \overline{x}^2} + O(\delta^2),$$

$$\text{(4.8)} \qquad \frac{\partial^2}{\partial y^2} = \frac{\partial^2}{\partial \overline{y}^2} - \delta \frac{\partial^2 \varphi}{\partial y^2} \frac{\partial}{\partial \overline{x}} - 2\delta \frac{\partial \varphi}{\partial y} \frac{\partial^2}{\partial \overline{x}\partial \overline{y}} + O(\delta^2).$$

We introduce the perturbed electric field and electron density as

$$\text{(4.9)} \qquad \mathbf{E} = E^{(0)} \mathbf{u}_x + \delta \left(E_x^{(1)} \mathbf{u}_x + E_y^{(1)} \mathbf{u}_y \right),$$

$$\text{(4.10)} \qquad n_e = n_e^{(0)} + \delta\, n_e^{(1)},$$
$$\text{(4.11)} \qquad n_p = n_p^{(0)} + \delta\, n_p^{(1)}.$$

For example, the perturbed electron density (4.10) reads

$$\text{(4.12)} \qquad n_e = n_e^{(0)} (x - \delta\varphi(x,y,t)) + \delta\, n_e^{(1)},$$

where $\varphi(x,y,t)$ is a purely geometrical perturbation and $\delta\, n_e^{(1)}$ is a perturbation of the electron density behind the front. Note that, in this sense, the kind of perturbation we are introducing is similar to the perturbations that are usually introduced in the study of the stability of other pattern-forming systems. This is the case, for instance, of the propagation of solidification fronts [13]. The difference here with respect to those other systems is the fact that our interface is not sharp but a boundary layer of thickness $\sqrt{D}$.

We shall assume here that $\varphi(x,y,0)$ is an initial perturbation independent of x. Note, at this point, that an x-dependence of the perturbation to the electron density is allowed in the term $n_e^{(1)}$.

4.1. Equations for the corrections at first order. Inserting these expressions into (2.9), we obtain

$$\frac{\partial n_e^{(0)}}{\partial \overline{t}} - E^{(0)} \frac{\partial n_e^{(0)}}{\partial \overline{x}} = n_e^{(0)}|E^{(0)}| + n_e^{(0)} \left(n_p^{(0)} - n_e^{(0)} \right)$$
$$+ D \left(1 - 2\delta \frac{\partial \varphi}{\partial x} \right) \frac{\partial^2 n_e^{(0)}}{\partial \overline{x}^2}$$
$$+ \delta \left[\frac{\partial \varphi}{\partial t} + E_x^{(1)} - E^{(0)} \frac{\partial \varphi}{\partial x} - D\,\Delta_{(x,y)}\varphi \right] \frac{\partial n_e^{(0)}}{\partial \overline{x}}$$
$$+ \delta \left(|E_x^{(1)}| + \left(n_p^{(1)} - n_e^{(1)} \right) \right) n_e^{(0)}$$
$$+ \delta \left(-\frac{\partial n_e^{(1)}}{\partial \overline{t}} + n_e^{(1)} \left(n_p^{(0)} - n_e^{(0)} \right) + E^{(0)} \frac{\partial n_e^{(1)}}{\partial \overline{x}} + n_e^{(1)}|E^{(0)}| \right)$$
$$\text{(4.13)} \qquad + \delta D\,\Delta_{(\overline{x},\overline{y})} n_e^{(1)} + O(\delta^2),$$

where $\Delta_{(x,y)} = \partial^2/\partial x^2 + \partial^2/\partial y^2$ and $\Delta_{(\overline{x},\overline{y})} = \partial^2/\partial \overline{x}^2 + \partial^2/\partial \overline{y}^2$. From (2.10) we obtain

$$(4.14) \quad \frac{\partial n_p^{(0)}}{\partial \overline{t}} + \delta \frac{\partial n_p^{(1)}}{\partial \overline{t}} = n_e^{(0)}|E^{(0)}| + \delta \frac{\partial \varphi}{\partial t}\frac{\partial n_p^{(0)}}{\partial \overline{x}} + \delta |E_x^{(1)}|n_e^{(0)} + \delta |E^{(0)}|n_e^{(1)} + O(\delta^2),$$

and from (2.11),

$$(4.15) \quad \frac{\partial E^{(0)}}{\partial \overline{x}} + \delta \left(\frac{\partial E_x^{(1)}}{\partial \overline{x}} + \frac{\partial E_y^{(1)}}{\partial \overline{y}} \right) = n_p^{(0)} - n_e^{(0)} + \delta \left(n_p^{(1)} - n_e^{(1)} \right) + \delta \frac{\partial \varphi}{\partial x}\frac{\partial E^{(0)}}{\partial \overline{x}} + O(\delta^2).$$

We can construct a solution up to $O(\delta^2)$ by imposing that $O(\delta^0)$ terms and $O(\delta^1)$ terms in (4.13), (4.14), and (4.15) vanish. The $O(\delta^0)$ terms give

$$(4.16) \quad \frac{\partial n_e^{(0)}}{\partial \overline{t}} = E^{(0)}\frac{\partial n_e^{(0)}}{\partial \overline{x}} + n_e^{(0)}|E^{(0)}| + n_e^{(0)}\left(n_p^{(0)} - n_e^{(0)} \right) + D\frac{\partial^2 n_e^{(0)}}{\partial \overline{x}^2},$$

$$(4.17) \quad \frac{\partial n_p^{(0)}}{\partial \overline{t}} = n_e^{(0)}|E^{(0)}|,$$

$$(4.18) \quad \frac{\partial E^{(0)}}{\partial \overline{x}} = n_p^{(0)} - n_e^{(0)},$$

and the $O(\delta^1)$ terms give

$$0 = \left[\frac{\partial \varphi}{\partial \overline{t}} + E_x^{(1)} - E^{(0)}\frac{\partial \varphi}{\partial \overline{x}} - D\,\Delta_{(\overline{x},\overline{y})}\varphi \right] \frac{\partial n_e^{(0)}}{\partial \overline{x}}$$

$$-2D\frac{\partial \varphi}{\partial \overline{x}}\frac{\partial^2 n_e^{(0)}}{\partial \overline{x}^2} + \left(|E_x^{(1)}| + n_p^{(1)} - n_e^{(1)} \right) n_e^{(0)}$$

$$-\frac{\partial n_e^{(1)}}{\partial \overline{t}} + n_e^{(1)}\left(n_p^{(0)} - n_e^{(0)} \right) + E^{(0)}\frac{\partial n_e^{(1)}}{\partial \overline{x}} + n_e^{(1)}|E^{(0)}|$$

$$(4.19) \qquad\qquad + D\,\Delta_{(\overline{x},\overline{y})}n_e^{(1)},$$

$$(4.20) \quad 0 = \frac{\partial n_p^{(1)}}{\partial \overline{t}} + \frac{1}{1 + 2\sqrt{D}}\frac{\partial \varphi}{\partial \overline{t}}n_e^{(0)} - |E_x^{(1)}|n_e^{(0)} - |E^{(0)}|n_e^{(1)},$$

$$(4.21) \quad 0 = \frac{\partial E_x^{(1)}}{\partial \overline{x}} + \frac{\partial E_y^{(1)}}{\partial \overline{y}} - \left(n_p^{(1)} - n_e^{(1)} \right) - \frac{\partial \varphi}{\partial \overline{x}}\left(n_p^{(0)} - n_e^{(0)} \right),$$

in which we have replaced, at order δ, derivatives with respect to x by derivatives with respect to $\overline{x}$, used (4.18) to replace $\partial E^{(0)}/\partial \overline{x}$ by $n_p^{(0)} - n_e^{(0)}$, and used (4.17), (3.29), and (3.30) to replace $\partial n_p^{(0)}/\partial \overline{x}$ by

$$(4.22) \quad \frac{\partial n_p^{(0)}}{\partial \overline{x}} = \frac{-1}{1 + 2\sqrt{D}}\frac{\partial n_p^{(0)}}{\partial \overline{t}} = \frac{-1}{1 + 2\sqrt{D}}n_e^{(0)}.$$

The solution of the system given by (4.16), (4.17), and (4.18) is the traveling wave found in the previous section so that

$$(4.23) \qquad\qquad n_e^{(0)} = f(\overline{\xi}),$$

where $\overline{\xi} = \overline{x} - c\overline{t}$.

In order to analyze the system (4.19)–(4.21), we introduce changes of coordinates in two stages: first, we change coordinates into a frame in which the planar front remains stationary and, second, we rescale coordinates in the boundary layer in order to make it of $O(1)$ size.

The first change of coordinates is of the form

(4.24)
$$x' = \bar{x} - c\bar{t}, \ y' = \bar{y}, \ t' = \bar{t},$$

where $c = 1 + 2\sqrt{D}$. Hence, the system (4.19)–(4.21) transforms into

$$0 = \left[\frac{\partial \varphi}{\partial t'} + E_x^{(1)} - D\,\Delta_{(x',y')}\varphi\right]\frac{\partial n_e^{(0)}}{\partial x'} - (E^{(0)} + c)\frac{\partial \varphi}{\partial x'}\frac{\partial n_e^{(0)}}{\partial x'}$$

$$-2D\frac{\partial \varphi}{\partial x'}\frac{\partial^2 n_e^{(0)}}{\partial x'^2} + \left(|E_x^{(1)}| + n_p^{(1)}\right)n_e^{(0)} - \frac{\partial n_e^{(1)}}{\partial t'} + (E^{(0)} + c)\frac{\partial n_e^{(1)}}{\partial x'}$$

(4.25)
$$+\left(|E^{(0)}| + n_p^{(0)} - 2n_e^{(0)}\right)n_e^{(1)} + D\,\Delta_{(x',y')}n_e^{(1)},$$

$$0 = \left(\frac{\partial}{\partial t'} - c\frac{\partial}{\partial x'}\right)n_p^{(1)} + \frac{1}{1 + 2\sqrt{D}}\left[\left(\frac{\partial}{\partial t'} - c\frac{\partial}{\partial x'}\right)\varphi\right]n_e^{(0)}$$

(4.26)
$$-|E_x^{(1)}|n_e^{(0)} - |E^{(0)}|n_e^{(1)},$$

(4.27) $$0 = \frac{\partial E_x^{(1)}}{\partial x'} + \frac{\partial E_y^{(1)}}{\partial y'} - \left(n_p^{(1)} - n_e^{(1)}\right) - \frac{\partial \varphi}{\partial x'}\left(n_p^{(0)} - n_e^{(0)}\right).$$

Second, noticing that x' is of order $\sqrt{D}$ at the boundary layer, as we saw in the previous section, we write

(4.28)
$$x' = \sqrt{D}\,\tilde{x}, \ y' = \sqrt{D}\,\tilde{y}, \ t' = \tilde{t}$$

to obtain the rescaled system

$$0 = \left[\frac{\partial \varphi}{\partial \tilde{t}} + E_x^{(1)} - \Delta_{(\tilde{x},\tilde{y})}\varphi\right]\frac{\partial n_e^{(0)}}{\partial \tilde{x}} - 2\frac{\partial \varphi}{\partial \tilde{x}}\frac{\partial^2 n_e^{(0)}}{\partial \tilde{x}^2}$$

$$-(E_{bl} + 2)\frac{\partial \varphi}{\partial \tilde{x}}\frac{\partial n_e^{(0)}}{\partial \tilde{x}} + \sqrt{D}\left(|E_x^{(1)}| + n_p^{(1)}\right)n_e^{(0)}$$

$$-\sqrt{D}\frac{\partial n_e^{(1)}}{\partial \tilde{t}} + \sqrt{D}(E_{bl} + 2)\frac{\partial n_e^{(1)}}{\partial \tilde{x}}$$

(4.29)
$$+\sqrt{D}\left(|E^{(0)}| + n_p^{(0)} - 2n_e^{(0)}\right)n_e^{(1)} + \sqrt{D}\,\Delta_{(\tilde{x},\tilde{y})}n_e^{(1)},$$

$$0 = \left(\frac{\partial}{\partial \tilde{t}} - \frac{c}{\sqrt{D}}\frac{\partial}{\partial \tilde{x}}\right)n_p^{(1)}$$

(4.30)
$$+\frac{1}{1 + 2\sqrt{D}}\left[\left(\frac{\partial}{\partial \tilde{t}} - \frac{c}{\sqrt{D}}\frac{\partial}{\partial \tilde{x}}\right)\varphi\right]n_e^{(0)} - |E_x^{(1)}|n_e^{(0)} - |E^{(0)}|n_e^{(1)},$$

(4.31) $$0 = \frac{\partial E_x^{(1)}}{\partial \tilde{x}} + \frac{\partial E_y^{(1)}}{\partial \tilde{y}} - \sqrt{D}\left(n_p^{(1)} - n_e^{(1)}\right) - \frac{\partial \varphi}{\partial \tilde{x}}\left(n_p^{(0)} - n_e^{(0)}\right),$$

where we have used that, at the boundary layer, by (3.32), $(E^{(0)} + c)/\sqrt{D} = E_{bl} + 2 + O(\sqrt{D})$.

The terms in (4.29) involving $n_e^{(1)}$ lead to a PDE for $n_e^{(1)}$. Namely,

(4.32) $$\frac{\partial n_e^{(1)}}{\partial \tilde{t}} - (E_{bl} + 2)\frac{\partial n_e^{(1)}}{\partial \tilde{x}} - \Delta_{(\tilde{x},\tilde{y})}n_e^{(1)} = \left(|E^{(0)}| + n_p^{(0)} - 2n_e^{(0)}\right)n_e^{(1)}.$$

Notice that (4.32) is an advection-diffusion equation with a source term of the form $(|E^{(0)}| + n_p^{(0)} - 2n_e^{(0)})n_e^{(1)}$. Since the source term is, from the expression for the

traveling waves found in subsection 3.2, negative behind the front, $n_e^{(1)}$ will decay exponentially fast, provided it lays in the ionized region, which is a basic assumption for our perturbation.

Hence, at leading order in (4.29), when $D \ll 1$, one obtains the equation

$$(4.33) \qquad 0 = \left[\frac{\partial \varphi}{\partial \tilde{t}} + E_x^{(1)} - \Delta_{(\tilde{x}, \tilde{y})} \varphi \right] \frac{\partial n_e^{(0)}}{\partial \tilde{x}} - 2 \frac{\partial \varphi}{\partial \tilde{x}} \frac{\partial^2 n_e^{(0)}}{\partial \tilde{x}^2} - (E_{bl} + 2) \frac{\partial \varphi}{\partial \tilde{x}} \frac{\partial n_e^{(0)}}{\partial \tilde{x}}.$$

Equation (4.31) is, at leading order in D,

$$(4.34) \qquad 0 = \frac{\partial E_x^{(1)}}{\partial \tilde{x}} + \frac{\partial E_y^{(1)}}{\partial \tilde{y}} - \frac{\partial \varphi}{\partial \tilde{x}} \left(n_p^{(0)} - n_e^{(0)} \right),$$

so that (4.33) and (4.34) are independent of $n_p^{(1)}$, and we can describe the evolution of the perturbed system as

$$(4.35) \qquad 0 = \frac{\partial \varphi}{\partial \tilde{t}} + E_x^{(1)} - \Delta_{(\tilde{x}, \tilde{y})} \varphi - 2 \frac{\partial \varphi}{\partial \tilde{x}} \frac{\partial^2 n_e^{(0)} / \partial \tilde{x}^2}{\partial n_e^{(0)} / \partial \tilde{x}} - (E_{bl} + 2) \frac{\partial \varphi}{\partial \tilde{x}},$$

$$(4.36) \qquad 0 = \frac{\partial E_x^{(1)}}{\partial \tilde{x}} + \frac{\partial E_y^{(1)}}{\partial \tilde{y}} - \frac{\partial \varphi}{\partial \tilde{x}} \left(n_p^{(0)} - n_e^{(0)} \right).$$

It will be more convenient for us to formulate (4.36) in terms of the electric potential in the next subsection.

4.2. The first order correction to the electric field. To establish conditions for the behavior of the perturbation of the electric field, we first note that the total electric field has to be irrotational since the magnetic field is negligible. So we will write $\mathbf{E} = -\nabla V$, where V is an electric potential. Then, (2.11) can be written as

$$(4.37) \qquad -\Delta_{(x,y)} V = n_p^{(0)} - n_e^{(0)} + \delta \, n_p^{(1)} + O(\delta^2).$$

Changing variables, we have

$$- \Delta_{(\overline{x}, \overline{y})} V + \delta \, \Delta_{(x,y)} \varphi \frac{\partial V}{\partial \overline{x}} + 2\delta \left(\frac{\partial \varphi}{\partial \overline{y}} \frac{\partial^2 V}{\partial \overline{x} \partial \overline{y}} + \frac{\partial \varphi}{\partial \overline{x}} \frac{\partial^2 V}{\partial \overline{x}^2} \right)$$

$$(4.38) \qquad = n_p^{(0)} - n_e^{(0)} + \delta \, n_p^{(1)} + O(\delta^2).$$

We write the electric potential as

$$(4.39) \qquad V(\overline{x}, \overline{y}) = V^{(0)}(\overline{x}) + \delta \, V^{(1)}(\overline{x}, \overline{y}),$$

so that (4.38) can be written, at the first two orders in δ, as

$$(4.40) \qquad -\frac{\partial^2 V^{(0)}(\overline{x})}{\partial \overline{x}^2} = n_p^{(0)} - n_e^{(0)},$$

$$(4.41) \qquad -\Delta_{(\overline{x}, \overline{y})} V^{(1)}(\overline{x}, \overline{y}) = -\Delta_{(\overline{x}, \overline{y})} \varphi \frac{\partial V^{(0)}(\overline{x})}{\partial \overline{x}} - 2 \frac{\partial \varphi}{\partial \overline{x}} \frac{\partial^2 V^{(0)}(\overline{x})}{\partial \overline{x}^2} + n_p^{(1)}.$$

Expression (4.40) implies that $V^{(0)}(\overline{x})$ is an electric potential associated with the electric field $E^{(0)}(\overline{x})$. The electric potential $V^{(1)}$ satisfies (4.41) with the condition of

decaying at $|\overline{x}| \to \infty$. Using (4.40) and (4.41), and the relation $E^{(0)} = -\partial V^{(0)}/\partial \overline{x}$, we arrive at

$$(4.42) \qquad -\Delta_{(\overline{x},\overline{y})}V^{(1)}(\overline{x},\overline{y}) = \Delta_{(\overline{x},\overline{y})}\varphi E^{(0)} + 2\frac{\partial\varphi}{\partial\overline{x}}\left(n_p^{(0)} - n_e^{(0)}\right) + n_p^{(1)}.$$

Changing coordinates as in (4.24) and (4.28), in terms of $(\tilde{x}, \tilde{y})$ coordinates that are $O(1)$ at the diffusion boundary layer, we obtain

$$- \Delta_{(\tilde{x},\tilde{y})}V^{(1)} = \left(\Delta_{(\tilde{x},\tilde{y})}\varphi\right)E^{(0)}(\sqrt{D}\tilde{x})$$

$$(4.43) \qquad +2\sqrt{D}\frac{\partial\varphi}{\partial\tilde{x}}\left(n_p^{(0)}(\sqrt{D}\tilde{x}) - n_e^{(0)}(\sqrt{D}\tilde{x})\right) + D\,n_p^{(1)}.$$

Neglecting $O(\sqrt{D})$ and $O(D)$ terms, and using (4.35), we can finally describe the evolution of the perturbed system as

$$(4.44) \qquad 0 = \frac{\partial\varphi}{\partial\tilde{t}} + E_x^{(1)} - \Delta_{(\tilde{x},\tilde{y})}\varphi - 2\frac{\partial\varphi}{\partial\tilde{x}}\frac{\partial^2 n_e^{(0)}/\partial\tilde{x}^2}{\partial n_e^{(0)}/\partial\tilde{x}} - (E_{bl} + 2)\frac{\partial\varphi}{\partial\tilde{x}},$$

$$(4.45) \qquad 0 = \Delta_{(\tilde{x},\tilde{y})}V^{(1)} + \left(\Delta_{(\tilde{x},\tilde{y})}\varphi\right)E^{(0)}(\sqrt{D}\tilde{x}).$$

In the following subsections we shall analyze the system (4.44)–(4.45).

4.3. Analysis of the perturbed system. It proves convenient, since the system (4.44)–(4.45) is linear, to use Fourier transforms in the coordinate $\tilde{y}$ (associated with the wave number k). Denoting the Fourier transform of function f as $\hat{f}$, we find

$$(4.46) \quad 0 = \frac{\partial\hat{\varphi}}{\partial\tilde{t}} + \hat{E}_x^{(1)} - \left(\frac{\partial^2\hat{\varphi}}{\partial\tilde{x}^2} - k^2\hat{\varphi}\right) - 2\frac{\partial\hat{\varphi}}{\partial\tilde{x}}\frac{\partial^2 n_e^{(0)}/\partial\tilde{x}^2}{\partial n_e^{(0)}/\partial\tilde{x}} - (E_{bl} + 2)\frac{\partial\hat{\varphi}}{\partial\tilde{x}},$$

$$(4.47) \quad 0 = \frac{\partial^2\hat{V}^{(1)}}{\partial\tilde{x}^2} - k^2\hat{V}^{(1)} + \left(\frac{\partial^2\hat{\varphi}}{\partial\tilde{x}^2} - k^2\hat{\varphi}\right)E^{(0)}(\sqrt{D}\tilde{x}),$$

a linear system that can be represented symbolically by

$$(4.48) \qquad \mathcal{L}(\hat{\varphi}, \hat{V}^{(1)}) = 0.$$

In principle, once $\hat{V}^{(1)}$ has been calculated from (4.47), we can calculate $\hat{E}_x^{(1)}$ as

$$(4.49) \qquad \frac{\partial\hat{V}^{(1)}}{\partial\overline{x}} = -\hat{E}_x^{(1)},$$

insert it into (4.46), and obtain an equation for $\hat{\varphi}$. Since $\hat{\varphi}$ is initially independent of $\tilde{x}$, we shall write

$$(4.50) \qquad \hat{\varphi} = \hat{\varphi}_0(k, t) + \hat{\varphi}_1(x, k, t),$$

with $\hat{\varphi}_1(x, k, t = 0) = 0$ and, accordingly,

$$(4.51) \qquad \hat{V}^{(1)} = \hat{V}_0^{(1)}(x, k, t) + \hat{V}_1^{(1)}(x, k, t).$$

We will require the following equations to be fulfilled: (i) for $\hat{\varphi}_0$ and $\hat{V}_0^{(1)}$,

$$(4.52) \qquad 0 = \frac{\partial\hat{\varphi}_0}{\partial\tilde{t}} + \hat{E}_{0x}^{(1)}(\tilde{x} = 0) + k^2\hat{\varphi}_0,$$

$$(4.53) \qquad 0 = \frac{\partial^2\hat{V}_0^{(1)}}{\partial\tilde{x}^2} - k^2\hat{V}_0^{(1)} - k^2\hat{\varphi}_0 E^{(0)}(\sqrt{D}\tilde{x}),$$

where

$$(4.54) \qquad \hat{E}_{0x}^{(1)} = -\frac{\partial \hat{V}_0^{(1)}}{\partial \overline{x}};$$

and (ii)

$$(4.55) \qquad \mathcal{L}(\hat{\varphi}_1, \hat{V}_1^{(1)}) = \begin{pmatrix} \hat{E}_{0x}^{(1)}(\tilde{x}=0,k,t) - \hat{E}_{0x}^{(1)}(\tilde{x},k,t) \\ 0 \end{pmatrix}$$

for $\hat{\varphi}_1$ and $\hat{V}_1^{(1)}$. We shall solve first (4.52)–(4.53) and proceed later to show that the φ_1 solution of (4.55) is merely a small perturbation of φ_0.

If we take the derivative of (4.53) with respect to $\overline{x}$, taking into account (4.49) and the relation between $E^{(0)} = -\partial V^{(0)}/\partial \overline{x}$ and $n_p^{(0)} - n_e^{(0)}$ given by (4.40), we find

$$(4.56) \qquad \frac{\partial^2 \hat{E}_{0x}^{(1)}}{\partial \tilde{x}^2} - k^2 \hat{E}_{0x}^{(1)} = -k^2 \hat{\varphi}_0 \left(n_p^{(0)}(\sqrt{D}\tilde{x}) - n_e^{(0)}(\sqrt{D}\tilde{x}) \right).$$

Taking the Fourier transform in $\tilde{x}$ (associated with the wave number ω) and denoting the double Fourier transform as $\hat{\hat{f}}$, one obtains

$$(4.57) \qquad (k^2 + \omega^2)\hat{\hat{E}}_{0x}^{(1)}(\omega,k) = \frac{k^2 \hat{\varphi}_0(k)}{\sqrt{2\pi}} \int_{-\infty}^{\infty} ds\, e^{-i\omega s} q(\sqrt{D}s),$$

where we have defined the net charge density as $q(\sqrt{D}\tilde{x}) = n_p^{(0)}(\sqrt{D}\tilde{x}) - n_e^{(0)}(\sqrt{D}\tilde{x})$. Taking the inverse Fourier transform in ω of (4.57), it follows that

$$
\begin{aligned}
\hat{E}_{0x}^{(1)}(\tilde{x},k) &= \frac{1}{2\pi} \int_{-\infty}^{\infty} d\omega\, e^{i\omega \tilde{x}} \frac{k^2 \hat{\varphi}_0(k)}{k^2 + \omega^2} \int_{-\infty}^{\infty} ds\, e^{-i\omega s} q(\sqrt{D}s) \\
(4.58) \qquad &= \frac{1}{2\pi} k^2 \hat{\varphi}_0(k) \int_{-\infty}^{\infty} ds\, q(\sqrt{D}s) \int_{-\infty}^{\infty} d\omega\, \frac{e^{i\omega(\tilde{x}-s)}}{k^2 + \omega^2}.
\end{aligned}
$$

The integral in ω can be done by deforming the integration contour in the complex plane. The result is

$$(4.59) \qquad \hat{E}_{0x}^{(1)}(\tilde{x},k) = \frac{|k|\hat{\varphi}_0(k)}{2} \int_{-\infty}^{\infty} ds\, q(\sqrt{D}s) e^{-|k|\,|\tilde{x}-s|}.$$

Since the value of $q = n_p^{(0)} - n_e^{(0)}$ in the case $D \ll 1$ differs from the same quantity in the case $D = 0$ only in the region of the boundary layer, that is, $O(D^{1/2})$, we can approximate the profile for the net charge density $q(\sqrt{D}\tilde{x})$ by the profile for the diffusionless traveling waves calculated in the previous section, i.e.,

$$(4.60) \qquad q(\sqrt{D}\tilde{x}) = \begin{cases} -e^{\sqrt{D}\tilde{x}} & \text{for } \tilde{x} < 0, \\ 0 & \text{for } \tilde{x} > 0. \end{cases}$$

With this approximation, (4.59) reads

$$(4.61) \qquad \hat{E}_{0x}^{(1)}(\tilde{x},k) = -\frac{|k|\hat{\varphi}_0(k)}{2} \int_{-\infty}^{0} ds\, e^{\sqrt{D}s} e^{-|k|\,|\tilde{x}-s|}.$$

The integral in (4.61) can be computed for both $\tilde{x} < 0$ and $\tilde{x} > 0$. The result is

$$(4.62) \qquad \hat{E}_{0x}^{(1)}(\tilde{x}, k) = -\frac{|k|\hat{\varphi}_0(k)}{2\sqrt{D}} \times \begin{cases} \frac{1}{1+|k|/\sqrt{D}} e^{-|k|\tilde{x}} & \text{for } \tilde{x} \geq 0, \\ \frac{-2|k|/\sqrt{D}}{1-|k|^2/D} e^{\sqrt{D}\tilde{x}} + \frac{1}{1-|k|/\sqrt{D}} e^{|k|\tilde{x}} & \text{for } \tilde{x} \leq 0. \end{cases}$$

Therefore,

$$(4.63) \qquad \hat{E}_{0x}^{(1)}(0, k) = -\frac{|k|\hat{\varphi}_0(k)}{2(\sqrt{D}+|k|)},$$

and

$$(4.64) \qquad R \equiv |\hat{E}_{0x}^{(1)}(\tilde{x} = 0, k, t) - \hat{E}_{0x}^{(1)}(\tilde{x}, k, t)| = O(e^{-|k|\tilde{x}} - 1)|\hat{\varphi}_0|.$$

Notice that

$$(4.65) \qquad R \leq |k\tilde{x}||\hat{\varphi}_0|,$$

a fact that we shall use below.

Let us remark that considering the profile of q with diffusion would change the integral in (4.61) by only an $O(1)$ amount, which is negligible in comparison with $1/(\sqrt{D}+|k|)$, provided $|k| \ll 1$.

4.4. The dispersion relation. Inserting the result (4.63) into (4.52), we find

$$(4.66) \qquad \frac{\partial\hat{\varphi}_0(k)}{\partial\tilde{t}} - \frac{|k|\hat{\varphi}_0(k)}{2(\sqrt{D}+|k|)} + |k|^2\hat{\varphi}_0(k) = 0.$$

Let us write the following ansatz for $\hat{\varphi}_0$:

$$(4.67) \qquad \hat{\varphi}_0(k, \tilde{t}) = e^{m\tilde{t}}\hat{\phi}(k).$$

Introducing this expression into (4.66), we obtain the relation

$$(4.68) \qquad m = \frac{|k|}{2(\sqrt{D}+|k|)} - |k|^2,$$

that is, the dispersion relation of the perturbations of the fronts. Note that there exists a maximum of $m(|k|)$ that selects the wavelength of the perturbation. It is easy to obtain the following expansion (in D) for the location of the maximum of m:

$$(4.69) \qquad k_{max} = \frac{1}{2^{2/3}}D^{1/6} - \frac{2}{3}D^{1/2} + \frac{2^{2/3}}{9}D^{5/6} + \frac{2^{7/3}}{81}D^{7/6} + O(D^{3/2}).$$

When D is a small parameter, this maximum is approximately located at

$$(4.70) \qquad k_{max} \approx \frac{D^{1/6}}{2^{2/3}}.$$

Notice that k_{max} is $O(D^{1/6})$ so that in the front, and for the fastest growing mode, where $\tilde{x} = O(1)$, we will have R defined in (4.64) of order $O(D^{1/6})|\hat{\varphi}_0|$.

Hence the solution to (4.55), with initial condition $\hat{\varphi}_1(\tilde{x}, k, 0) = 0$, will be such that $|\hat{\varphi}_1| = O(D^{1/6})t$ and will constitute merely a small perturbation of the leading

order $\hat{\varphi}_0$. In fact, $\hat{\varphi}_1$ will be a small perturbation of $\hat{\varphi}_0$ whenever $|k| \ll 1$ and not only in the neighborhood of the fastest growing mode.

The value of k_{max} in (4.70) corresponds to a typical spacing between fingers in the coordinate y given by

$$(4.71) \qquad \lambda_{max} = \frac{2\pi D^{1/2}}{k_{max}} \approx 10\, D^{1/3}.$$

In the original nondimensional quantities, this is

$$(4.72) \qquad \lambda_{max} \approx 10 \left(\frac{D_e}{\mathcal{E}_\infty} \right)^{1/3}.$$

The typical spacing can be put into physical quantities for nitrogen using the relations (1.9), (1.10), and (1.15). In this way, we can give the dependence of the physical spacing λ^d between consecutive fingers in terms of the gas pressure p (in bars), the physical external electric field $\mathcal{E}_\infty^d$, and the diffusion coefficient D_e^d. We obtain

$$\lambda_{max}^d \approx 10 R_0 \left(\frac{\mathcal{E}_0}{D_0} \right)^{1/3} \left(\frac{D_e^d}{\mathcal{E}_\infty^d} \right)^{1/3}$$

$$(4.73) \qquad \approx 2.3 \times 10^{-5}\,\mathrm{m} \left(\frac{2 \times 10^7\,\mathrm{V} \cdot bar/\mathrm{m}}{1.8\,\mathrm{m}^2/\mathrm{s}} \right)^{1/3} \left(\frac{D_e^d}{p\,\mathcal{E}_\infty^d} \right)^{1/3}$$

so that the spacing decreases as the gas pressure or the external electric field increases, and increases as the diffusion coefficient increases. This expression shows the possibility of validating the main results of this work through experiments of electric discharges in nitrogen.

5. Numerical studies of stability of planar fronts and nonplanar waves. The theory developed in the previous sections applies solely to waves traveling at velocity $c = 1$ in the nondiffusive case and $c = 1 + 2\sqrt{D}$ when $D \neq 0$. These traveling waves appear only for a certain class of initial data, namely, those for which n_e is identically zero beyond a certain point in space. From the numerical point of view, solutions tend to develop traveling waves which do not propagate exactly with that velocity. Nevertheless, we will show in this numerical section that the main stability/instability features of our theoretical results remain valid in general. Specifically, we show the existence of traveling waves in the form of fingers when the diffusion coefficient is small enough, and show that for a given diffusion coefficient, stability of planar fronts depends critically on the wavelength of the perturbations.

We developed a numerical code to solve the initial value problem and study the evolution of nonplanar traveling waves. We discretized the equations with finite differences on a domain of size $L_x \times L_y$ with a uniform square grid of spacing h. For the temporal integration we used an improved Euler scheme. We first compute an approximation for the solution of the system (2.9)–(2.11) at $t + \delta t/2$ as

$$(5.1) \qquad \Delta_a \phi^{(k)} = -(n_p - n_e)^{(k)},$$

$$(5.2) \qquad n_e^{(k+1/2)} = n_e^{(k)} + \frac{\delta t}{2} \left(\mathbf{E} \cdot \nabla_u n_e + n_e(n_p - n_e) + D + \Delta_a n_e + n_e |\mathbf{E}| \right)^{(k)},$$

$$(5.3) \qquad n_p^{(k+1/2)} = n_p^{(k)} + \frac{\delta t}{2} \left(n_e |\mathbf{E}| \right)^{(k)},$$

and then we obtain a second order approximation by using the derivatives at the center of the interval $(t, t + \delta t)$,

(5.4) $\Delta_a \phi^{(k+1/2)} = - (n_p - n_e)^{(k+1/2)}$,

(5.5) $n_e^{(k+1)} = n_e^{(k)} + \delta t \left(\mathbf{E} \cdot \nabla_c n_e + n_e (n_p - n_e) + D \Delta_a n_e + n_e |\mathbf{E}| \right)^{(k+1/2)}$,

(5.6) $n_p^{(k+1)} = n_p^{(k)} + \delta t \left(n_e |\mathbf{E}| \right)^{(k+1/2)}$,

where the superscript (k) denotes the time step at time $k\delta t$, $\mathbf{E} = -\nabla_c \phi$, and

$$\Delta_a \phi = \frac{1}{6h^2} [\phi_{i+1,j+1} + \phi_{i+1,j-1} + \phi_{i-1,j+1} + \phi_{i-1,j-1}$$

(5.7)
$$+ 4(\phi_{i+1,j}\phi_{i-1,j} + \phi_{i,j+1} + \phi_{i,j-1}) - 20\phi_{ij}]$$

is the second order accurate approximation of the Laplacian that is symmetrical up to third order. In (5.2) and (5.5), ∇_u is the upwind gradient with respect to the electric field, and ∇_c is the centered second order accurate gradient. In order to solve the Poisson equations (5.1) and (5.4), we used successive overrelaxations (SOR) [3], which in our case is convenient because at each time step we have a good approximation of the solution from the previous step.

We found empirically that the scheme is stable, provided we satisfy the following CFL-like condition:

(5.8) $\delta t < \min(h/(2E_m), h^2/4D)$,

where E_m is the maximum value of the absolute value of the electric field in the domain of integration (which in our equations plays the role of velocity).

We enforce the following boundary conditions:

(5.9) $\dfrac{\partial \phi}{\partial x}(L_x, y) = 1$, $\phi(0, y) = 0$, $\dfrac{\partial \phi}{\partial y}(x, L_y) = \dfrac{\partial \phi}{\partial y}(x, 0) = 0$,

(5.10) $n_e(L_x, y) = \dfrac{\partial n_e}{\partial x}(0, y) = 0$, $\dfrac{\partial n_e}{\partial y}(x, L_y) = \dfrac{\partial n_e}{\partial y}(x, 0) = 0$,

(5.11) $n_p(L_x, y) = \dfrac{\partial n_p}{\partial x}(0, y) = 0$, $\dfrac{\partial n_p}{\partial y}(x, L_y) = \dfrac{\partial n_p}{\partial y}(x, 0) = 0$,

which correspond to a constant electric field on the top end of the domain and zero-flux conditions on the sides.

5.1. Validation with traveling waves. We validated the scheme by comparing the numerical solution with the following exact solutions for the traveling waves without diffusion:

(5.12) $n_e^{ex}(\zeta) = 1 - \dfrac{e^\zeta}{\sqrt{e^\zeta(4 + e^\zeta)}}$,

$n_p^{ex}(\zeta) = 1 + \dfrac{e^\zeta}{2} - \dfrac{e^{\zeta/2}\sqrt{4 + e^\zeta}}{2} + \dfrac{\log 2}{2}$

(5.13) $- \log \left(e^{\zeta/2} + \sqrt{4 + e^\zeta} \right) + \dfrac{1}{2} \log \left(2 + e^\zeta + e^{\zeta/2}\sqrt{4 + e^\zeta} \right)$,

where $\zeta = x - 2t$. This solution is convenient for the validation because it is smooth, and our numerical scheme is best suited to calculating differentiable solutions. We
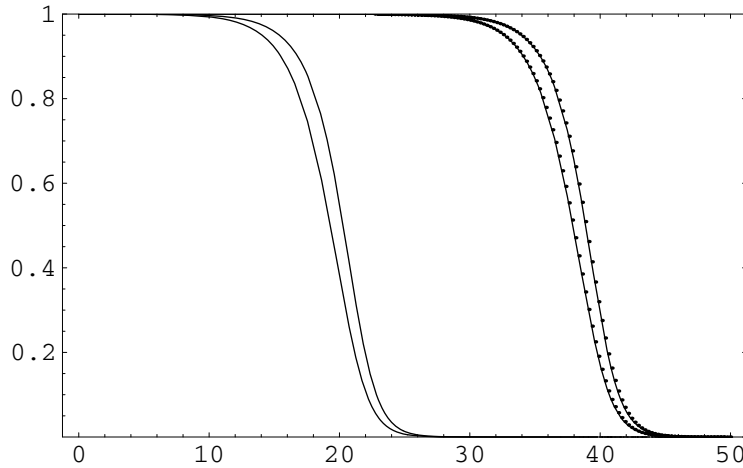
FIG. 3. *Validation with an explicit solution for $c = 2$ and $D = 0$. The size of the domain is $L_x = 50$ and we used 200 gridpoints. The curves on the left indicate the initial condition for n_e (upper line) and n_p (lower line), and the curves on the right show the comparison between the numerical calculation and the exact solution at $t = t_q$.*

first set as an initial condition the exact solution at $t = 0$ and then we compute the numerical solution at $t_q = 9.5$. In Figure 3 we show the comparison between both solutions. In Figure 4 we show the total error calculated as

$$(5.14) \qquad \text{error} = \int_0^{L_x} \left(n_e(x, t_q) - n_e^{ex}(x, t_q) \right)^2 dx.$$

This measure of error takes into account the accumulation of all arithmetic and truncation errors on the time interval $(0, t_q)$. Figure 4 shows that the error is proportional to the square of the interspacing h, indicating that the scheme is second order accurate.

5.2. Computing two-dimensional traveling waves. One difficulty that arises with a finite computational domain is that traveling waves eventually arrive at the end of the domain of integration. This is a problem because, given an arbitrary initial condition, sometimes it takes a long time for traveling waves to converge to a steady state.

We solve this difficulty by making use of a displacement technique that keeps the waves near the center of the domain at all times. Each time that the position of the front of a wave (defined, for example, as the point where $n_e = 0.1$) is beyond the middle of the domain, we then translate the solution backwards by exactly one gridpoint,

$$(5.15) \qquad n_{e i,j} \leftarrow n_{e i+1,j}, \qquad n_{p i,j} \leftarrow n_{p i+1,j}.$$

At the end of the domain $(i = n_x)$ we set zero values for the charge densities. Using this procedure, we can compute two-dimensional traveling waves. In the following calculations, we have $\lambda = 10$, $L_y = 2\lambda$, $L_x = 3L_y$ and the domain is discretized by 300×100 points. The initial condition has a plane front perturbed with a cosenoidal perturbation of wavelength λ and amplitude $\lambda/40$.
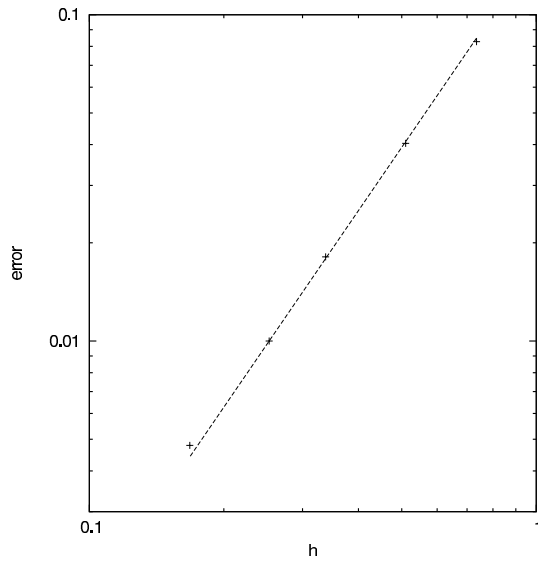
FIG. 4. *Errors integrated along the domain of integration for $D = 0$ at time $t_q = 9.5$. The size of the domain is $L = 50$ and we used 200 gridpoints. The points indicate the resulting numerical errors, and the line is a power with exponent 2, indicating that the scheme is second order accurate.*
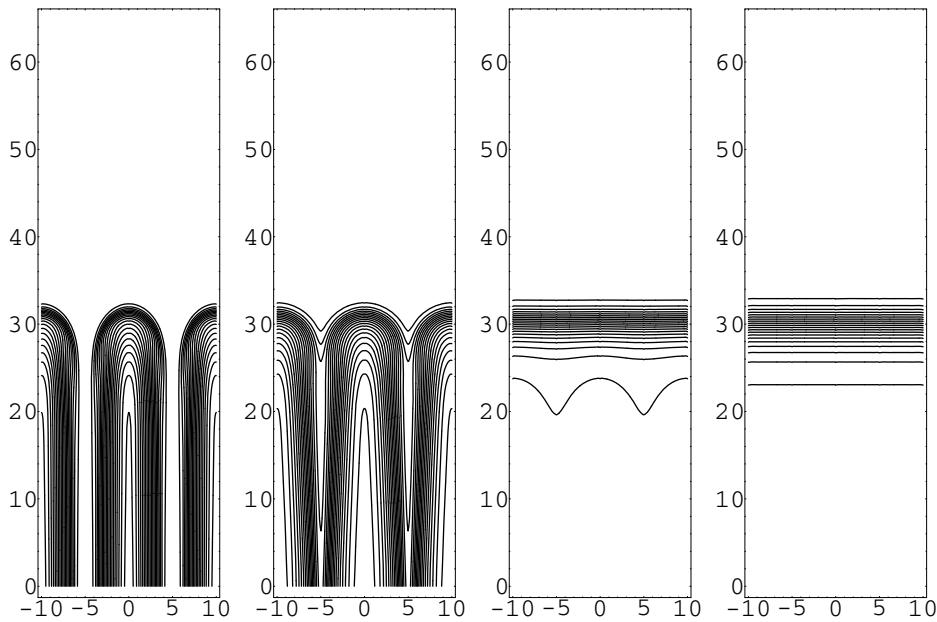

FIG. 5. *Two-dimensional contour plots for the electronic charge density for the traveling waves with $D = 0$, 0.1, 0.2, and 0.3. The x-axis is in the vertical direction.*
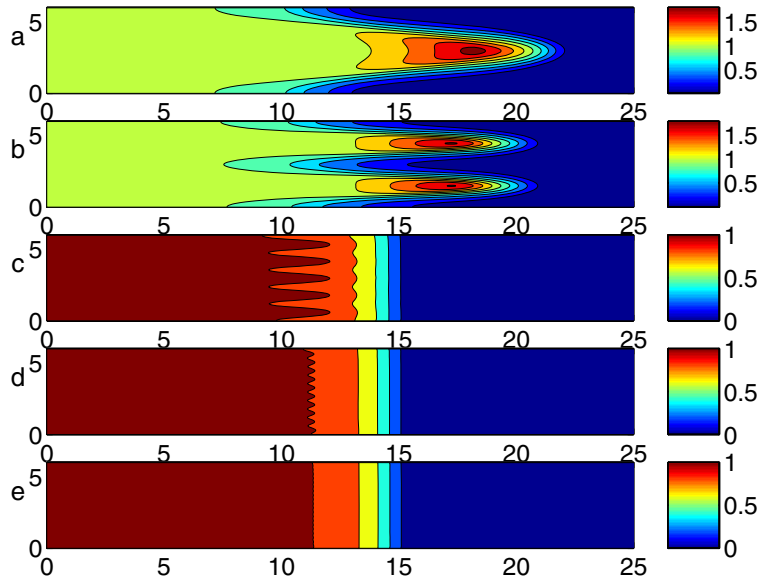
FIG. 6. *Level curves of the electron density n_e with diffusion coefficient $D = 0.1$ and time interval 2. The wavelength of the perturbation is, in each case, (a) $\lambda = 6$, (b) $\lambda = 3$, (c) $\lambda = 5/6$, (d) $\lambda = 10/6$, and (e) $\lambda = 20/6$. These values correspond to wave numbers $k = 2\pi/\lambda$.*

We observed that after the wave travels a distance equivalent to ten times the length of the computational domain, the numerical solution reaches a steady state, which is insensitive to the initial conditions. In Figure 5 we show traveling waves with $D = 0$, 0.1, 0.2, and 0.3. Notice that the aspect of the traveling waves is very sensitive to the value of the diffusion coefficient. In particular, when D is close to zero, well-developed fingers do appear, while the fronts remain essentially planar when D is large enough.

In Figure 6 we perturb a planar traveling wave, which was found with the displacement procedure described above. The perturbation was introduced by translating all the contour lines a distance $\cos(2\pi y/\lambda)$ on the x-direction. Then we evolved the solution on a time interval of length 2. In all cases $D = 0.1$, and we take several wavelengths λ. It is evident from the figures that there is a tendency to form fingers when the wavelength is above some critical value while the perturbation decays and disappears for small enough wavelengths. In Figure 7, the cases (b) and (c) of Figure 6 have been plotted in perspective. This confirms the results obtained in previous sections concerning stability.

6. Conclusions. In this paper we have used a fluid approximation to describe the process of electric breakdown in nonattaching gases such as nitrogen. We have shown that a planar negative front separating an ionized region from a region without charge may become unstable under the combined action of the external electric field and the electron diffusion. The common underlying mathematical structure allows us to exploit some of the ideas developed for other pattern-forming systems such as the Hele–Shaw and Stefan problems.

We have calculated the dispersion relation for a perturbation in the transversal direction of a planar traveling wave in the limit of small diffusion. An analytical expression for the typical spacing between fingers is obtained.
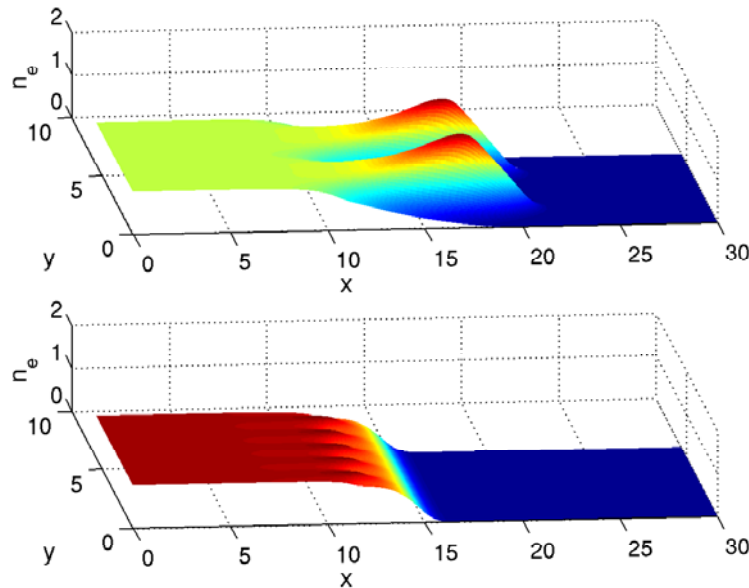
Fig. 7. *Representations in perspective of the electron density in the cases* (b) *and* (c) *of Figure* 6, *respectively.*

In order to test the analytical results, we have developed a numerical code to study the evolution of planar traveling waves. The traveling waves are then perturbed and we follow the evolution after that. Under some circumstances the solutions converge to traveling waves in the form of fingers that we have computed numerically for several diffusion coefficients. Our numerical results clearly support the conclusions on the branching and stability developed analytically.

REFERENCES

[1] N. D. ALIKAKOS, P. W. BATES, AND X. CHEN, *The convergence of solutions of the Cahn-Hilliard equation to the solution of Hele-Shaw model*, Arch. Ration. Mech. Anal., 128 (1994), pp. 165–205.
[2] S. M. ALLEN AND J. W. CAHN, *A macroscopic theory for antiphase boundary motion and its application to antiphase domain coarsening*, Acta. Metal., 27 (1979), pp. 1085–1095.
[3] W. F. AMES, *Numerical Methods for Partial Differential Equations*, 3rd ed., Academic Press, New York, 1992.
[4] M. ARRAYÁS, U. EBERT, AND W. HUNDSDORFER, *Spontaneous branching of anode-directed streamers between planar electrodes*, Phys. Rev. Lett., 88 (2002), article 174502.
[5] M. ARRAYÁS AND U. EBERT, *Stability of negative ionization fronts: Regularization by electric screening?*, Phys. Rev. E, 69 (2004), article 036214.
[6] M. ARRAYÁS, M. A. FONTELOS, AND J. L. TRUEBA, *Power laws and self-similar behavior in negative ionization fronts*, J. Phys. A: Math. Gen., 39 (2006), pp. 7561–7578.
[7] M. ARRAYÁS, M. A. FONTELOS, AND J. L. TRUEBA, *Photoionization effects in ionization fronts*, J. Phys. D: Appl. Phys., 39 (2006), pp. 5176–5182.

[8] M. ARRAYÁS, M. A. FONTELOS, AND J. L. TRUEBA, *Mechanism of branching in negative ionization fronts*, Phys. Rev. Lett., 95 (2005), article 165001.

[9] M. ARRAYÁS AND J. L. TRUEBA, *Investigations of pre-breakdown phenomena: Streamer discharges*, Cont. Phys., 46 (2005), pp. 265–276.

[10] J. W. CAHN AND J. E. HILLIARD, *Free energy of a nonuniform system* I: *Interfacial free energy*, J. Chem. Phys., 28 (1958), pp. 258–351.

[11] E. N. DANCER, D. HILHORST, M. MIMURA, AND L. A. PELETIER, *Spatial segregation limit of a competition-diffusion system*, European J. Appl. Math., 10 (1999), pp. 97–115.

[12] U. EBERT, W. VAN SAARLOOS, AND C. CAROLI, *Propagation and structure of planar streamer fronts*, Phys. Rev. E, 55 (1997), pp. 1530–1549.

[13] C. GODRÈCHE, ED., *Solids Far from Equilibrium*, Cambridge University Press, Cambridge, UK, 1991.

[14] A. N. KOLMOGOROV, I. G. PETROVSKII, AND N. S. PISKUNOV, *Study of the diffusion equation with growth of the quantity of matter and its application to a biology problem*, in Selected Works of A. N. Kolmogorov, Vol. I, Kluwer Academic, Amsterdam, 1991, pp. 242–270.

[15] N. LIU AND V. P. PASKO, *Effects of photoionization on propagation and branching of positive and negative streamers in sprites*, J. Geophys. Res., 109 (2004), pp. 1–17.

[16] J. D. MURRAY, *Mathematical Biology*, Springer-Verlag, New York, 1990.

[17] V. P. PASKO, M. A. STANLEY, J. D. MATHEWS, U. S. INAN, AND T. G. WOOD, *Electrical discharge from a thundercloud top to the lower ionosphere*, Nature, 416 (2002), pp. 152–154.

[18] Y. P. RAIZER, *Gas Discharge Physics*, Springer, Berlin, 1991.

[19] J. RUBINSTEIN, P. STERNBERG, AND J. B. KELLER, *Fast reaction, slow diffusion, and curve shortening*, SIAM J. Appl. Math., 49 (1989), pp. 116–133.